

CA 8608385

AECL-8902

ATOMIC ENERGY
OF CANADA LIMITED



L'ÉNERGIE ATOMIQUE
DU CANADA LIMITÉE

COMPUTED TOMOGRAPHY OF DRILL CORES

**Evaluation des carottes de forage
par tomographie informatisée**

T. TAYLOR

Chalk River Nuclear Laboratories

Laboratoires nucléaires de Chalk River

Chalk River, Ontario

August 1985 août

ATOMIC ENERGY OF CANADA LIMITED

COMPUTED TOMOGRAPHY OF DRILL CORES

by

T. Taylor

Instrument Development Branch
Chalk River Nuclear Laboratories
Chalk River, Ontario K0J 1J0
1985 August

AECL-8902

L'ENERGIE ATOMIQUE DU CANADA, LIMITEE

Evaluation des carottes de forage par tomographie informatisée

par

T. Taylor

Résumé

Une évaluation préliminaire, par tomographie informatisée, de carottes de forage provenant de masses de granite et de grès a permis d'obtenir d'importantes données géologiques. Les variations de densité aussi faibles que 4% et les fractures pouvant n'avoir que 0,1 mm de largeur ont été facilement détectées.

Département de développement des instruments
Laboratoires nucléaires de Chalk River
Chalk River, Ontario K0J 1J0

Août 1985

ATOMIC ENERGY OF CANADA LIMITED

COMPUTED TOMOGRAPHY OF DRILL CORES

by

T. Taylor

ABSTRACT

A preliminary computed tomography evaluation of drill cores of granite and sandstone has generated geologically significant data. Density variations as small as 4% and fractures as narrow as 0.1 mm were easily detected.

Instrument Development Branch
Chalk River Nuclear Laboratories
Chalk River, Ontario K0J 1J0
1985 August

AECL-8902

TABLE OF CONTENTS

	<u>Page</u>
1. INTRODUCTION	1
2. PROCEDURE	1
3. RESULTS AND DISCUSSION	1
4. CONCLUSIONS	6
5. ACKNOWLEDGMENTS	12
6. REFERENCES	12

1. INTRODUCTION

Drill cores play a crucial role in modern geology. Even though they are acquired at substantial expense and are often irreplaceable, they are destroyed by most of the accepted examination techniques. Needless to say, the geological community is interested in nondestructive methods of evaluation, and, in particular, in techniques for the quantification of fractures and variations in density. Computed tomography appears to be ideally suited to the task. This report presents a preliminary evaluation of the use of computed tomography to examine drill cores of both igneous and sedimentary rock.

2. PROCEDURE

Images were generated with a first generation CT system (1) comprised of a ^{137}Cs radioisotopic source, a NaI (Tl) scintillation detector and a computer controlled stage that rotated and translated a drill core through the gamma-ray beam. Both the source and the detector were equipped with tungsten alloy collimators 1.6 mm wide by 3.2 mm high by 165 mm long, generating a photon beam with a full-width-at-half-maximum of approximately 0.9 mm. One hundred and eighty projections were measured at 1.0° intervals spanning an arc of 180° . The projections were sampled at 128 discrete points separated by 0.5 mm. The total duration of a complete scan was 55 h. (The throughput can be increased significantly as discussed in section 4.). The images were reconstructed by filtered back projection (2) of linearly interpolated projections with a Ramachandran - Lakshminarayanan filter (3). A pixel size of 0.5 mm was used.

Each of the resultant images was enhanced by histogram equalization (4). (Histogram equalization generates a grey scale such that there are an equal number of pixels at every grey level, thus making optimum use of the dynamic range of the visual system).

A total of three images were obtained, as follows:

- a) a radial slice of a pink medium grained granite core with numerous epidote filled fractures (see Fig. 1)
- b) a radial slice of a grey fine grained sandstone core with a conspicuous fracture (see Fig. 2), and
- c) an axial slice of a piece of the sandstone core (see Fig. 3).

The granite and the sandstone cores were both 45 mm in diameter.

3. RESULTS AND DISCUSSION

All of the images had an in-plane spatial resolution of approximately 1.0 mm and a contrast resolution of about 2%.

The image of the granite drill core is shown in Fig. 4. The linear attenuation coefficient is, for the most part, $0.20 \pm 0.01 \text{ cm}^{-1}$; however, there are small regions with a somewhat greater linear attenuation coefficient of $0.22 \pm 0.01 \text{ cm}^{-1}$. Assuming a mass attenuation coefficient of $0.077 \text{ cm}^2 \cdot \text{g}^{-1}$ (5), the

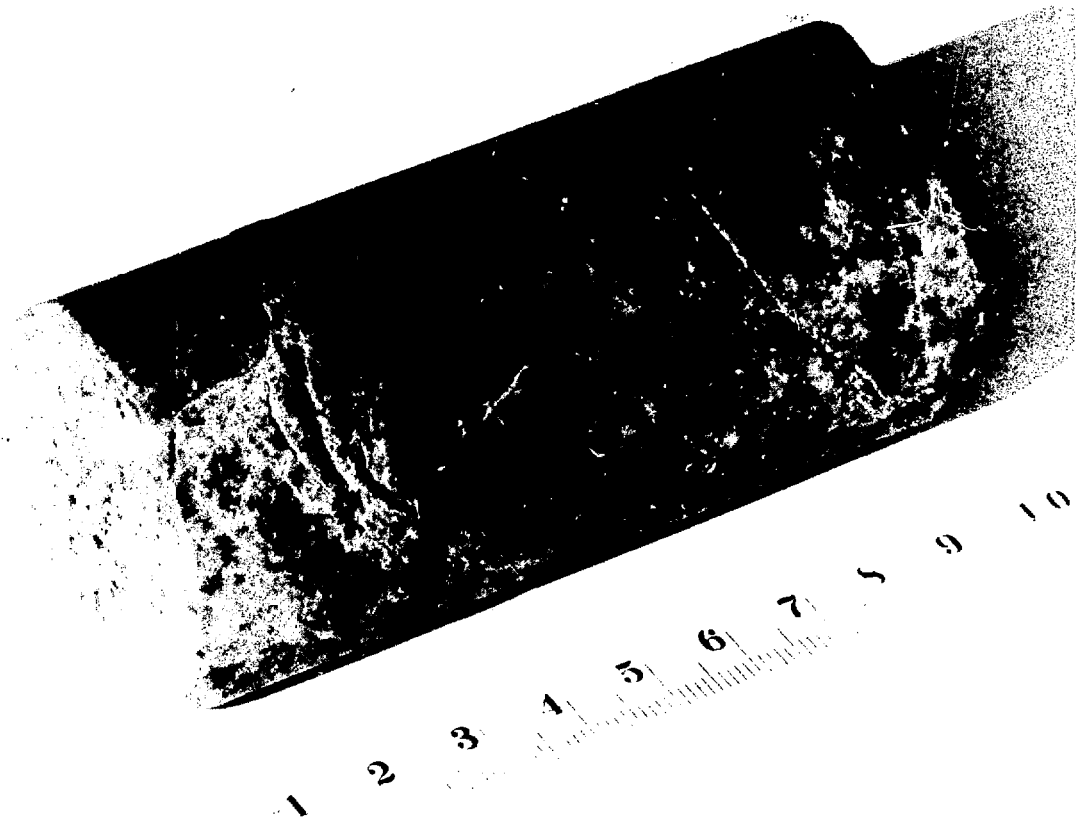


Figure 1: Granite drill core. The black line locates the imaged slice.

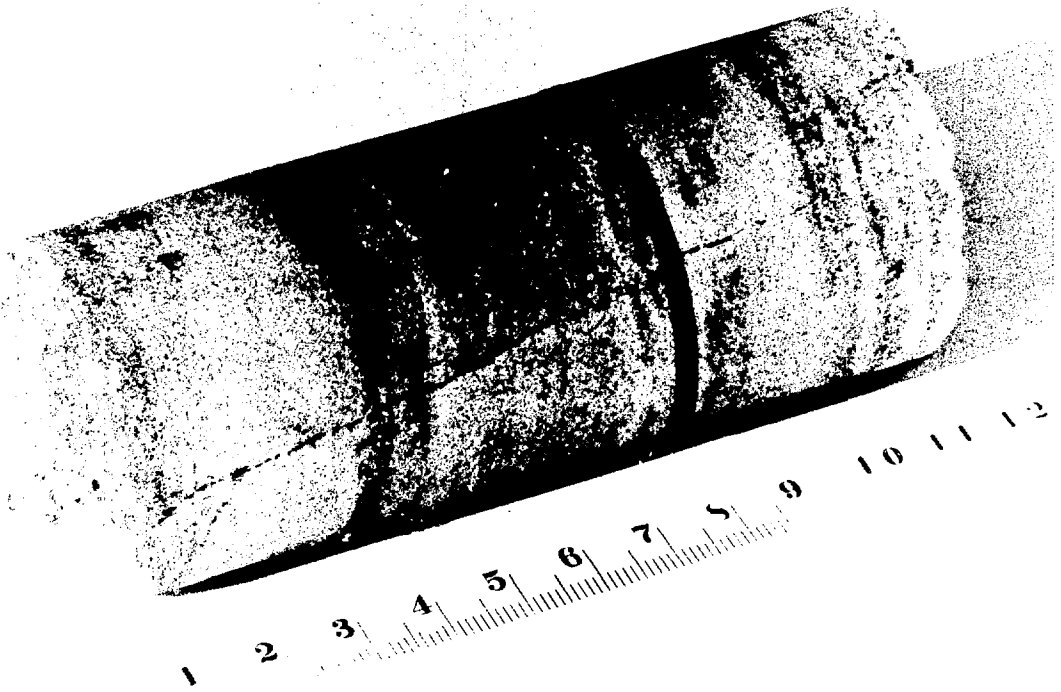


Figure 2: Sandstone drill core. The black line locates the imaged slice.

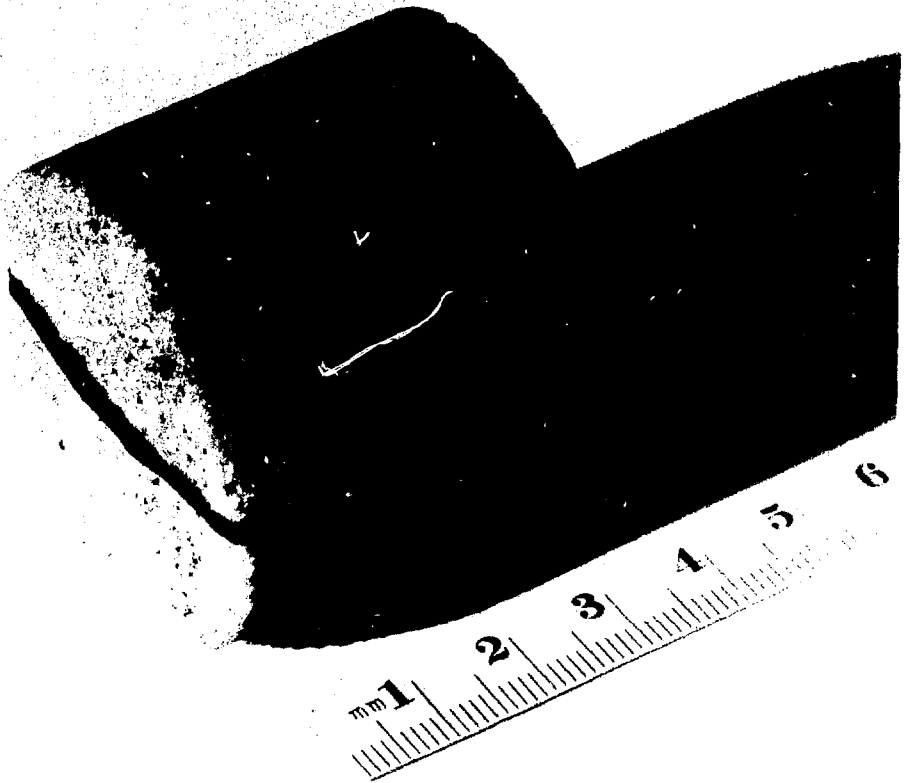


Figure 3: Part of the sandstone drill core. The black line locates the imaged axial slice.

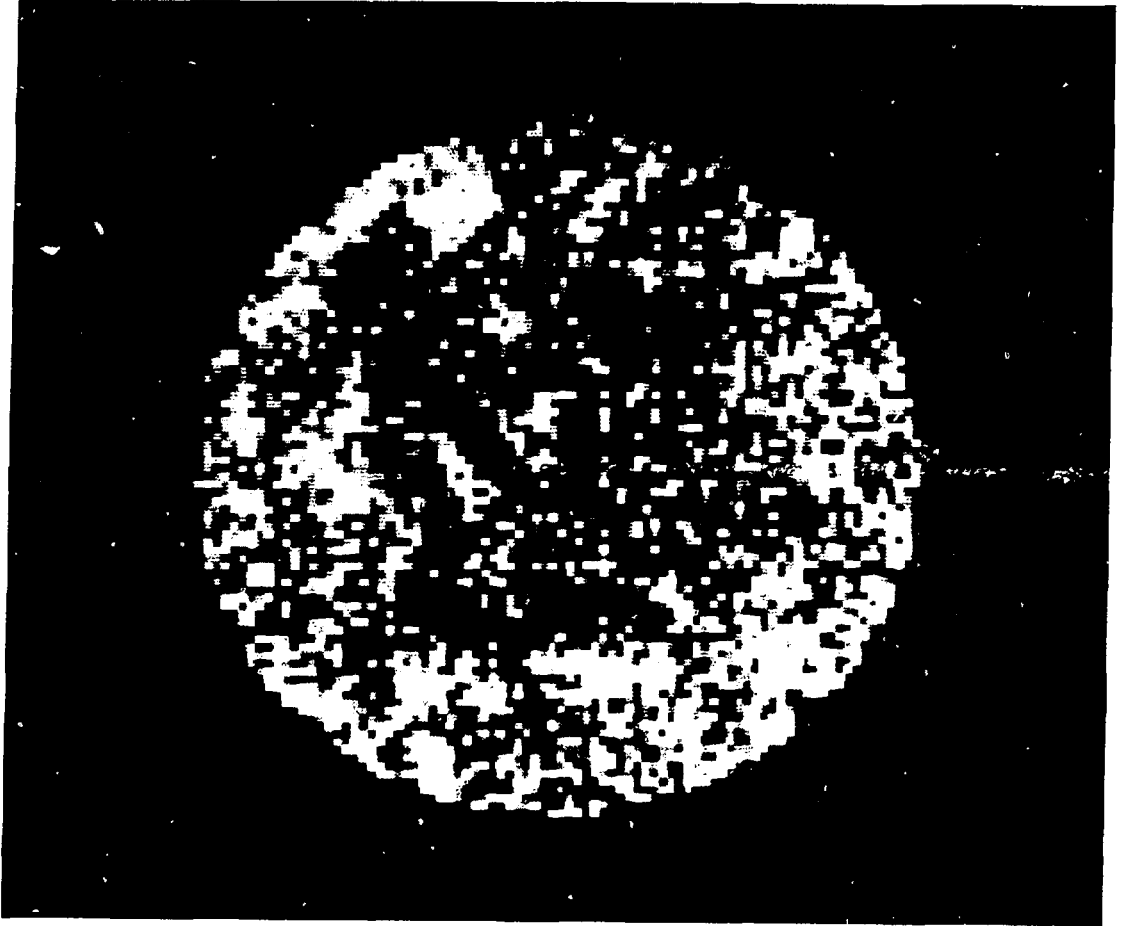


Figure 4: Computed tomography image of the granite drill core. Black represents low attenuation, white is high attenuation.

corresponding densities are $2.6 \pm 0.1 \text{ g}\cdot\text{cm}^{-3}$ and $2.9 \pm 0.1 \text{ g}\cdot\text{cm}^{-3}$. Granite is comprised principally of quartz and orthoclase with a density of $2.60 \text{ g}\cdot\text{cm}^{-3}$ and plagioclase with density of 2.60 to $2.76 \text{ g}\cdot\text{cm}^{-3}$ (6). However, ferromagnesium minerals with a density of 2.80 to $3.40 \text{ g}\cdot\text{cm}^{-3}$ are usually present in lesser amounts. These probably account for the regions of higher attenuation. The epidote filled fractures were neither wide enough nor of sufficiently different density to be detected.

The radial image of the sandstone drill core is shown in Fig. 5. Although visual inspection of the core suggested a single fracture, the computed tomography image revealed what appears to be a pair of fractures running from the lower left to the upper right. Figure 6 shows attenuation profiles that pass through the hypothetical fractures. Assuming that the slight variations in the attenuation correspond to air filled fractures, a fracture width of approximately 0.1 mm is inferred (7). The core was subsequently sectioned (see Fig. 7) confirming the above interpretation.

Apart from the fractures, the radial sandstone image had a uniform attenuation of $0.19 \pm 0.01 \text{ cm}^{-1}$ corresponding to a density of $2.5 \pm 0.1 \text{ g}\cdot\text{cm}^{-3}$. The density of sandstone varies with the deposition mechanism and, to a lesser extent, the composition (6). The density observed here is at the upper end of the normal range.

The axial image of the sandstone core (see Fig. 8) again revealed the fractures at the top centre, but, in addition, layers running horizontally across the image became apparent. Figure 9 shows a horizontal attenuation profile passing through the fractures and a vertical profile passing through the layers. Some of the layers have a linear attenuation coefficient of $0.20 \pm 0.01 \text{ cm}^{-1}$, rather than $0.19 \pm 0.01 \text{ cm}^{-1}$, corresponding to a density of $2.6 \pm 0.1 \text{ g}\cdot\text{cm}^{-3}$, rather than $2.5 \pm 0.1 \text{ g}\cdot\text{cm}^{-3}$. Although this may be due to differences in deposition conditions, the colour differences apparent in Figs 2,3 and 7 suggest variations in composition.

A detailed analysis of the axial image revealed a high-density inclusion near the bottom of the crack. The inclusion has a linear attenuation coefficient of $0.21 \pm 0.01 \text{ cm}^{-1}$ corresponding to a density of $2.8 \text{ g}\cdot\text{cm}^{-3}$ and may be a flake of granite.

4. CONCLUSIONS

It has been demonstrated that computed tomography can generate geologically significant data. The resource sector could benefit from this nondestructive imaging technique in both research and exploration.

The throughput would obviously have to be increased significantly, especially for field work. Fortunately, the imaging time can easily be reduced by at least five orders of magnitude. Since the optimum energy in this case is about 110 keV (8), an x-ray tube can be substituted for the relatively low-intensity radioisotopic source that was used in this study. A further increase in throughput could be achieved by replacing the single detector used here with an array of hundreds of

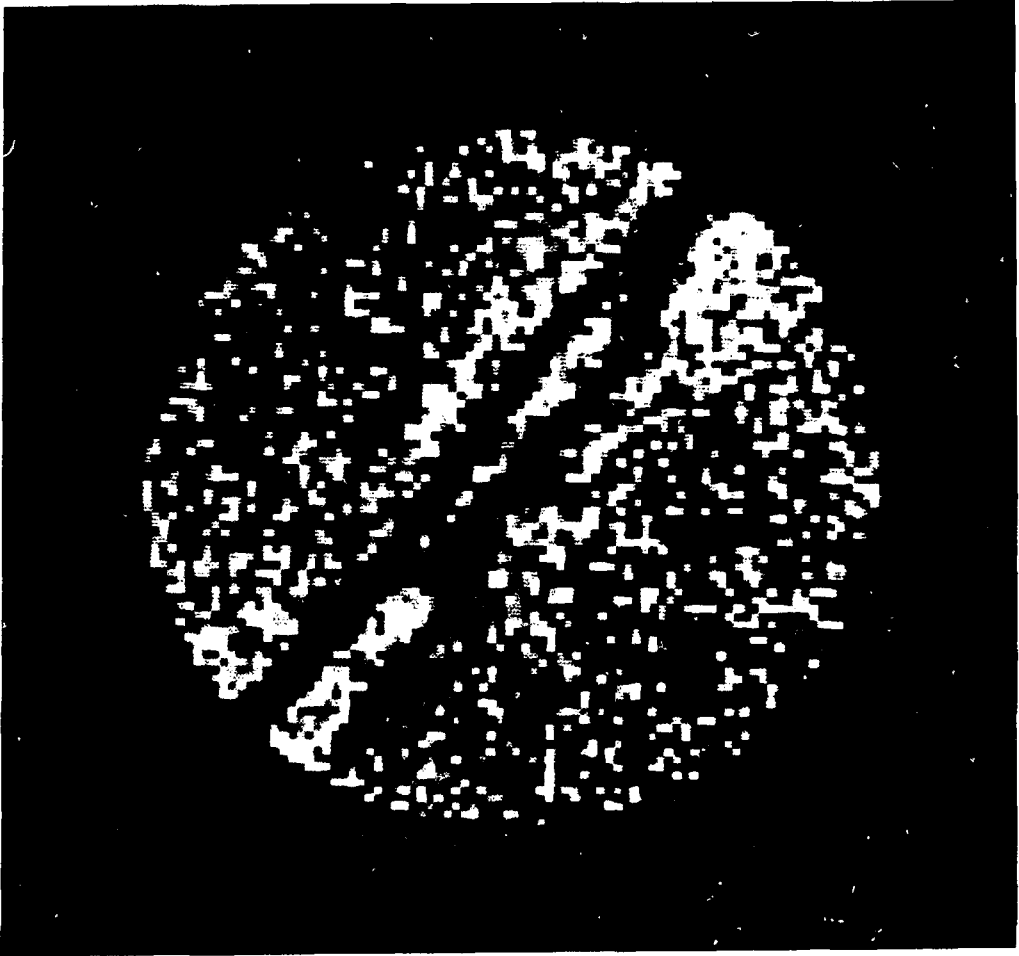


Figure 5: Radial computed tomography image of the sandstone drill core. Black represents low attenuation, white is high attenuation.

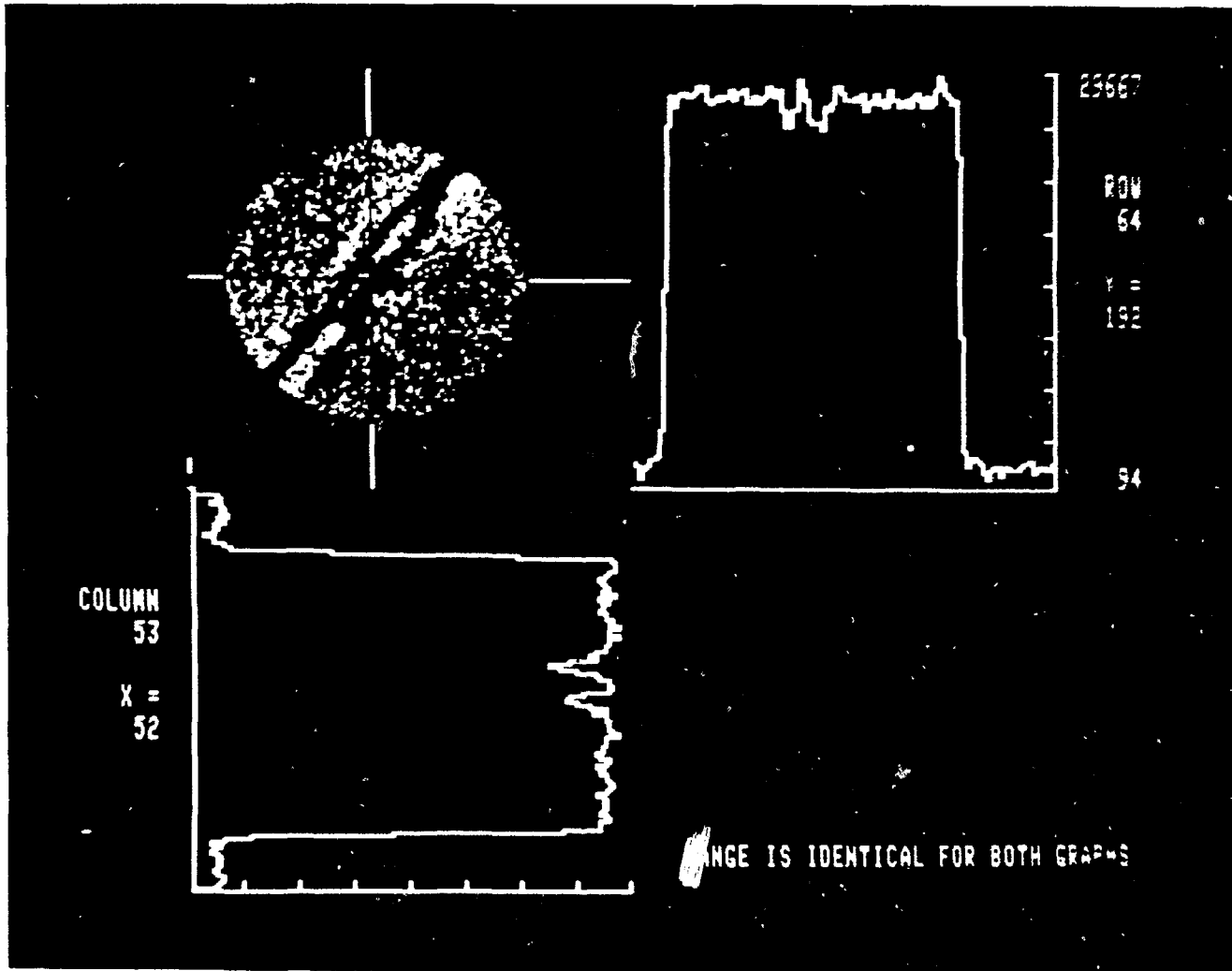


Figure 6: Horizontal (upper right) and vertical (lower left) attenuation profiles for the radial computed tomography image of the sandstone drill core.



Figure 7: Sandstone drill core sectioned at the imaged slice

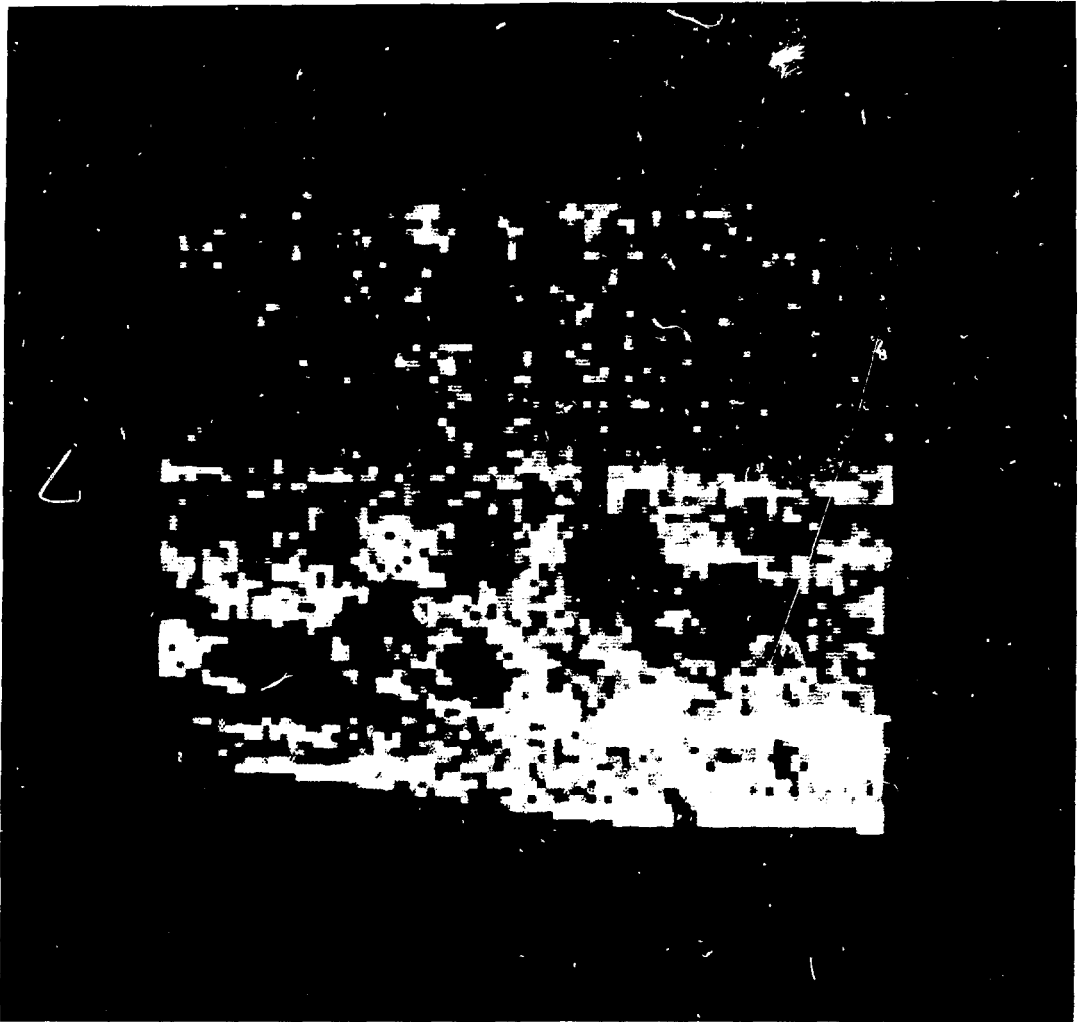


Figure 8: Axial computed tomography image of part of the sandstone drill core. Black represents low attenuation; white is high attenuation.

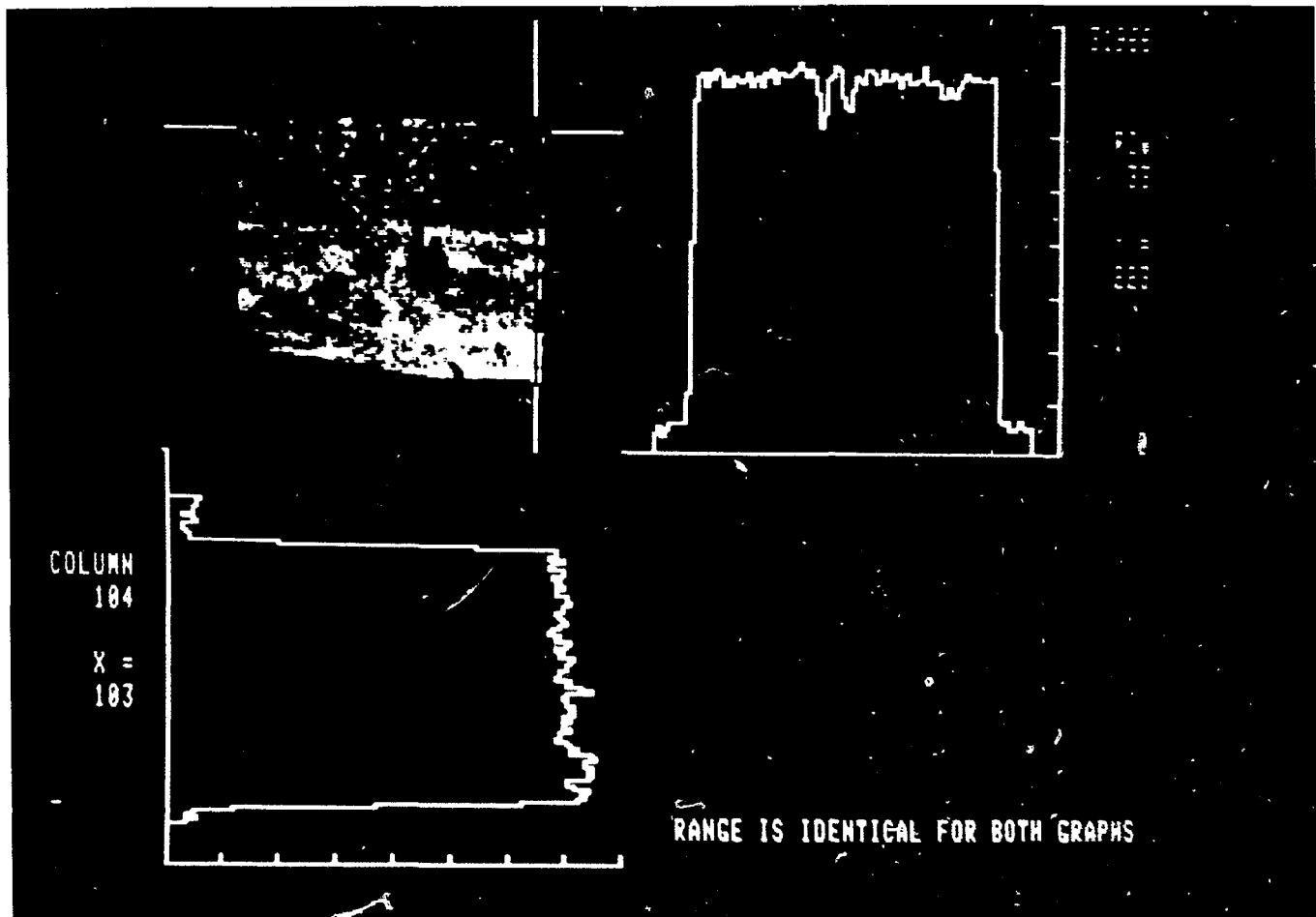


Figure 9: Horizontal (upper right) and vertical (lower left) attenuation profiles for the axial computed tomography image of part of the sandstone drill core.

detectors.

It is also worth noting that axial images, which probably will prove more useful than radial images, can be generated without sectioning the core. A sequence of radial images can be rebinned to generate any number of axial slices (9).

5. ACKNOWLEDGMENTS

The author wishes to thank P.W. Reynolds and G. Tosello for helping to operate the computed tomography system, L.R. Lupton for assisting with the image reconstruction, and J. Dugal of the Geological Survey of Canada for submitting the samples.

6. REFERENCES

- (1) P.D. Tonner and G. Tosello, "An Industrial Application of Computer Assisted Tomography: Detection, Location and Sizing of Shrink Cavities in Valve Castings", Atomic Energy of Canada Ltd. Report AECL-8626 (1984).
- (2) A.C. Kak, "Computerized Tomography with X-ray Emission and Ultrasound Sources", Proc. IEEE 69 (1979) 1245.
- (3) G.N. Ramachandran and A.V. Lakshminarayanan, "Three Dimensional Reconstruction from Radiographs and Electron Micrographs: Application of Convolutions Instead of Fourier Transforms", Proc. Natl. Acad. Sci. USA, 68 (1971) 2236.
- (4) R.C. Gonzalez and P. Wintz, "Digital Image Processing" (Addison - Wesley Publishing Co., London, 1977).
- (5) E. Storm and H.I. Israel, "Photon Cross-Sections from 1 keV to 100 MeV for Elements 1 through 100", Nucl. Data, A7 (1970) 565.
- (6) D.F. Hewitt and E.B. Freeman, "Rocks and Minerals of Ontario", (Ontario Department of Mines and Northern Affairs, Toronto, 1972)
- (7) T. Taylor, "The Sizing of Cracks and Voids by Computed Tomography" Atomic Energy of Canada Ltd. Report (In preparation).
- (8) L. Grodzins, "Optimum Energies for X-Ray Transmission Tomography of Small Samples", Nucl. Instr. and Meth 206 (1983) 541.
- (9) L.R. Lupton, "An Industrial Application of Computer Assisted Tomography: Three Dimensional Mapping of a Motorcycle Carburetor", Atomic Energy of Canada Ltd. Report AECL-8829 (1985).

ISSN 0067 - 0367

To identify individual documents in the series we have assigned an AECL- number to each.

Please refer to the AECL- number when requesting additional copies of this document

from

Scientific Document Distribution Office
Atomic Energy of Canada Limited
Chalk River, Ontario, Canada
K0J 1J0

Price \$2.00 per copy

ISSN 0067 - 0367

Pour identifier les rapports individuels faisant partie de cette série nous avons assigné un numéro AECL- à chacun.

Veillez faire mention du numéro AECL- si vous demandez d'autres exemplaires de ce rapport

au

Service de Distribution des Documents Officiels
L'Énergie Atomique du Canada Limitée
Chalk River, Ontario, Canada
K0J 1J0

Prix \$2.00 par exemplaire

©ATOMIC ENERGY OF CANADA LIMITED, 1985